Modelling current transfer to cathodes in metal halide plasmas

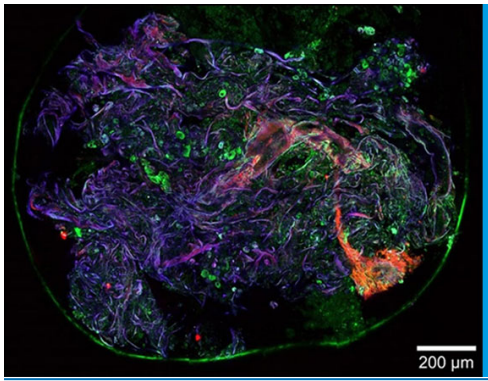

INSTITUTE OF PHYSICS PUBLISHING JOURNAL OF PHYSICS D: APPLIED PHYSICS

J. Phys. D: Appl. Phys. **38** (2005) 3155–3162 doi:10.1088/0022-3727/38/17/S16

Modelling current transfer to cathodes in metal halide plasmas

M S Benilov[1], M D Cunha[1] and G V Naidis[2]

[1] Departamento de Física, Universidade da Madeira, Largo do Município, 9000 Funchal, Portugal

[2] Institute for High Temperatures of the Russian Academy of Sciences, Izhorskaya 13/19, Moscow 125412, Russia

Received 22 February 2005, in final form 2 May 2005
Published 19 August 2005
Online at stacks.iop.org/JPhysD/38/3155

Abstract

This work is concerned with investigation of the main features of current transfer to cathodes under conditions characteristic of metal halide (MH) lamps. It is found that the presence of MHs in the gas phase results in a small decrease of the cathode surface temperature and of the near-cathode voltage drop in the diffuse mode of current transfer; the range of stability of the diffuse mode expands. Effects caused by a variation of the work function of the cathode surface owing to formation of a monolayer of alkali metal atoms on the surface are studied for particular cases where the monolayer is composed of sodium or caesium. It is found that the formation of the sodium monolayer affects the diffuse mode of current transfer only moderately and in the same direction that the presence of metal atoms in the gas phase affects it. Formation of the caesium monolayer produces a dramatic effect: the cathode surface temperature decreases very strongly, the diffuse-mode current–voltage characteristic becomes N–S-shaped.

1. Introduction

The model of nonlinear surface heating has become a widely accepted tool for modelling plasma–cathode interaction in high-pressure arc discharge devices; see works [1–12] and references therein. The model was validated [4, 13] by a detailed comparison with the experiment.

In this work, this model is used for establishing the main features of current transfer to cathodes under conditions characteristic of metal halide (MH) lamps. The presence of MHs affects the current transfer in two ways: through variation of properties of the near-cathode plasma layer owing to the presence of MHs in the gas phase, and through variation of the work function of the cathode surface owing to formation of an alkali metal monolayer on the surface. Both effects are studied in this work.

The outline of the paper is as follows. The model of near-cathode layer in MH plasmas is developed in section 2. In section 3, variation of the work function of the cathode surface owing to formation of a monolayer of sodium or caesium atoms on the surface is discussed. Results of simulations of a diffuse discharge on tungsten cathodes and of its stability are given in section 4.

2. Near-cathode layer in MH plasmas

An important constituent of the model of interaction of a high-pressure plasma with a refractory cathode is a model of the near-cathode plasma layer. Such a model has been developed in preceding works for the case of a plasma composed of atoms of a single species, ions of a single species and electrons [4, 6, 14]. (A summary of the model [4, 6, 14] can be found on the internet [15], as well as an online tool for simulation of plasma–cathode interaction based on this model.) In [16], the latter model was generalized for the case of a plasma with multiple ion and neutral species by introducing a number of effective coefficients, the most important of them being the effective rate constant of ionization of a neutral particle by electron impact and the effective mean cross-section for momentum transfer in elastic collisions between a positive ion and a neutral particle. The effective coefficients are evaluated by averaging the corresponding individual coefficients over plasma composition evaluated at the plasma edge of the ionization layer. The plasma composition at the edge of the ionization layer is found by solving equations of local balance of production and loss of every plasma species in volume reactions for given elementary

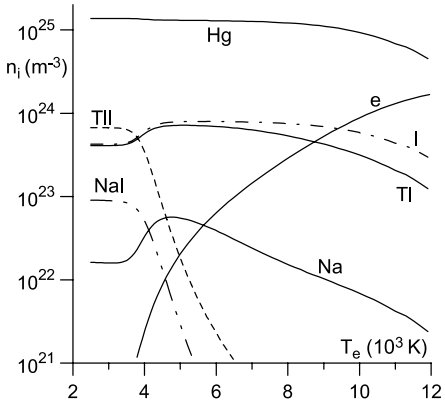

Figure 1. Densities of neutral plasma species at the edge of the ionization layer in the MH plasma versus the electron temperature. Hg : Na : Tl : I = 0.89 : 0.005 : 0.05 : 0.055, $p = 5$ bar, $T_h = 2500$ K.

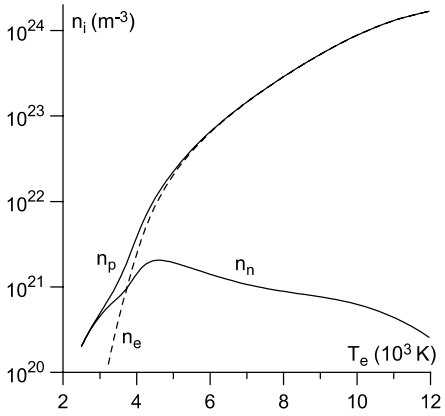

Figure 2. Densities of positive ions n_p, negative ions n_n and electrons n_e versus the electron temperature. Hg : Na : Tl : I = 0.89 : 0.005 : 0.05 : 0.055, $p = 5$ bar, $T_h = 2500$ K.

composition of the mixture and given values of the heavy-particle (gas) temperature T_h, electron temperature T_e and gas pressure p. Note that there is no detailed balancing between direct and reverse reactions at the edge of the ionization layer, therefore, a calculation of the plasma composition requires, in addition to thermodynamic data, also kinetic data (in contrast to the case of an LTE plasma in which $T_h = T_e$). The aim of this section is to apply the model [16] to the plasma of MH lamps.

The plasma-producing gas in MH lamps represents a mixture of molecular and atomic species composed of Hg and (some of) the following elements: Hg, Na, Tl, Dy, Sc, Cs, I and Ar. The neutral species taken into account in this work are Hg, Na, Tl, Cs, Dy, Sc, I, NaI, TlI, CsI, DyI, DyI_2, DyI_3, ScI, ScI_2, ScI_3. Ion species produced in ionization of atoms are Hg^+, Na^+, Tl^+, Dy^+, Sc^+, Cs^+, I^+. As the ionization potentials of metal iodides are substantially higher than those of corresponding metal atoms (e.g. 5.14 eV for Na and 7.54 eV for NaI, 6.11 eV for Tl and 8.47 eV for TlI, 3.89 eV for Cs and 7.25 eV for CsI), the presence of molecular ions is neglected. Attachment of electrons to atoms I results in the appearance of ions I^-. The model includes, in particular, an account of dissociation of metal iodide molecules by impact of both neutral particles and electrons. The presence of Ar atoms is disregarded, since their density is much smaller than the density of mercury atoms while their ionization potential is higher.

As an example, results of calculations for the mixture with elementary composition Hg : Na : Tl : I = 0.89 : 0.005 : 0.05 : 0.055 (which approximately corresponds to the chemical composition at low temperatures Hg : NaI : TlI = 0.945 : 0.005 : 0.05) and $p = 5$ bar are presented in this work. Densities of neutral plasma species at the edge of the ionization layer are given in figure 1 as functions of T_e, the electron temperature for $T_h = 2500$ K. Under equilibrium conditions, at $T_e = T_h$, the densities of free metal atoms are smaller than the densities of metal iodides. As T_e increases, iodides get dissociated in collisions with electrons.

Densities of positive ions, negative ions and electrons versus the electron temperature are shown in figure 2. In the range $T_e \gtrsim 4000$ K, the density of negative ions is much smaller than that of electrons; hence, the presence of negative ions in the mixture can be neglected and the model of the near-cathode plasma layer developed in [4, 6, 14] is applicable.

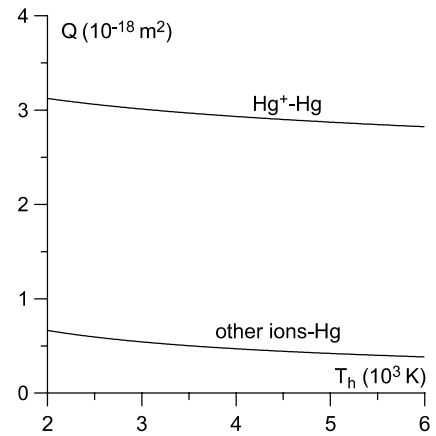

Figure 3. Mean cross-sections of momentum transfer in collisions of ions Hg^+ and of ions of the other species with Hg atoms.

Mercury atoms are a dominating neutral species under conditions of interest for MH lamps, hence, one can neglect contributions of other neutral species while calculating the effective mean cross-section of momentum transfer in collisions between ions and neutral particles. Collisions of ions Na^+, Tl^+, Dy^+, Sc^+, Cs^+ and I^+ with atoms Hg are governed by the polarization interaction. The mean cross-section of momentum transfer in such collisions is independent of ion species. Collisions of Hg^+ with Hg are governed by charge transfer. Mean cross-sections of ion–atom collisions of MH plasma species determined in such a way are shown in figure 3.

The effective mean cross-section of momentum transfer in collisions between ions and neutral particles, calculated on the basis of the above-described data versus the electron temperature, is shown in figure 4. At low T_e, the dominating ion species are those which have low ionization potential (Na^+, Tl^+, Cs^+, Dy^+, Sc^+), so the effective cross-section is close to the cross-section of collisions of ions other than Hg^+ with Hg atoms. At high T_e, the dominating ion species is Hg^+ (ions of the most abundant species) and the effective cross-section approaches the cross-section of collisions Hg^+–Hg. The change of ion composition starts at T_e around 6000 K.

The rate constants of ionization of atoms Hg, Na, Tl, Dy, Sc, Cs, I by electron impact have been calculated with

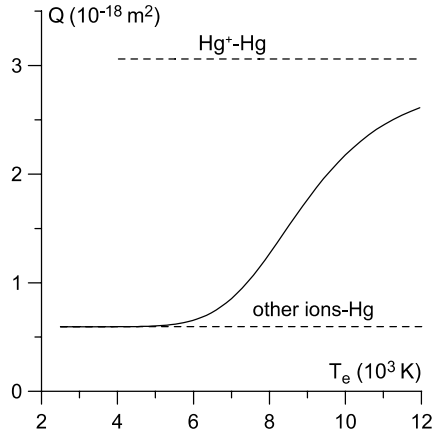

Figure 4. Effective mean cross-section of momentum transfer in the MH plasma versus the electron temperature (——). Hg : Na : Tl : I =0.89 : 0.005 : 0.05 : 0.055, $p = 5$ bar, $T_h = 2500$ K. (– – –) mean cross-sections of momentum transfer in collisions of ions others than Hg^+ with Hg atoms and in collisions Hg^+–Hg.

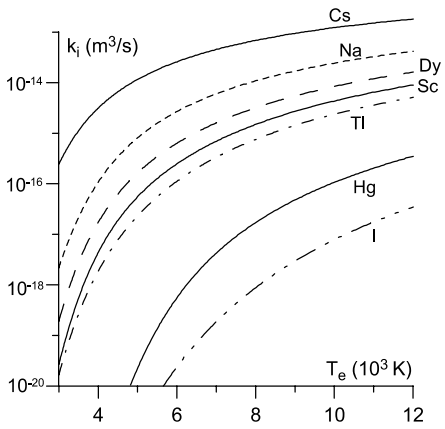

Figure 5. Ionization rate constants of atomic species of MH plasmas.

the use of the modified diffusion approximation [17] and are shown in figure 5. The effective ionization rate constant versus the electron temperature is shown in figure 6. Also shown in figure 6 is the rate constant of ionization of mercury atoms. At low T_e, when the ionization degrees of all atomic species are small, the dominating ionization process is given by ionization of atoms with low ionization potentials (Na, Tl, Cs, Dy, Sc) and the effective ionization rate constant exceeds considerably the ionization rate constant of mercury atoms. At high T_e, the dominating ionization process is the ionization of the most abundant atomic species (mercury) when the two curves approach each other.

3. Work function of a surface covered by a monolayer of alkali atoms

In order to identify effects caused by a variation of the work function of the cathode surface owing to formation of a monolayer of alkali metal atoms on the surface, a particular case will be considered where the plasma-producing gas contains mercury and one alkali metal, namely sodium or caesium. As will be seen later, this selection allows one

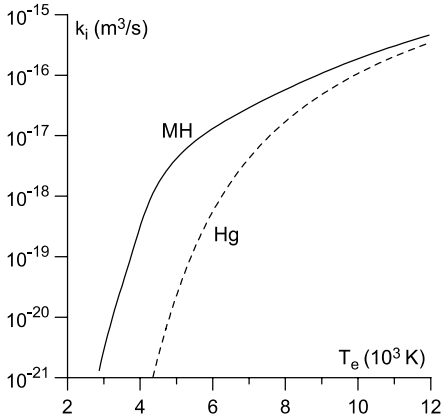

Figure 6. The effective ionization rate coefficient in the MH plasma versus the electron temperature (——). Hg : Na : Tl : I = 0.89 : 0.005 : 0.05 : 0.055, $p = 5$ bar, $T_h = 2500$ K. (– – –) the ionization rate constant of Hg atoms.

to illustrate both a situation in which the variation of the work function affects the plasma–cathode interaction only moderately and a situation in which it brings about new effects which dramatically change the plasma–cathode interaction. Also, the Na–Hg plasma merits independent interest with reference to high-pressure sodium lamps.

Parameters governing the work function for such systems are the partial pressure of the alkali metal and the temperature of the cathode surface. For convenience, molar fraction of the alkali metal in the mixture, Z_{Na} or Z_{Cs}, will be specified instead of its partial pressure. Then, the partial pressure of Na or Cs is calculated in terms of the molar fraction as $Z_{Na}p$ or, respectively, $Z_{Na}p$, where p is the total pressure of the mixture (which, again, was set equal to 5 bar). The work function was evaluated with the use of semi-empirical formulae presented in [18] and [19] for Na–Hg and Cs–Hg plasmas, respectively.

The dependence of the work function on the temperature T_w of the cathode surface is as follows. The work function A_f is governed by θ, the surface coverage (fraction of the surface which is covered with alkali atoms), which, in turn, is governed by the partial pressure of alkali atoms and the temperature of the cathode surface. At $\theta \ll 1$, when the cathode surface is effectively clean of alkali atoms, A_f takes the value corresponding to tungsten, which is 4.55 eV. At θ close to unity, A_f takes the value corresponding to the alkali metal, which is about 2.6 eV for Na and about 2.2 eV for Cs. At θ intermediate between 0 and 1, the dependence $A_f(\theta)$ is non-monotonic and takes a minimum value at a certain $\theta = \theta_m$; note that $\theta_m \approx 0.7$, $A_f(\theta_m) \approx 2.1$ eV for Na [18] and $\theta_m \approx 0.5$, $A_f(\theta_m) \approx 1.6$ eV for Cs [19].

The surface coverage is governed by the condition of equilibrium between the alkali atoms in the gas phase and those bound to the surface, that is, by the condition of equality of adsorption and desorption (evaporation) rates. With increase in the temperature, the desorption rate increases exponentially, while the rate of adsorption is much weaker. As a result, the surface coverage monotonously decreases with an increase of T_w at a fixed partial pressure of atoms, from $\theta \approx 1$ at low T_w to $\theta \ll 1$ at high T_w. Given the above-described non-monotony of the dependence $A_f(\theta)$, one concludes that the dependence of the work function on the cathode surface temperature is also non-monotonic.

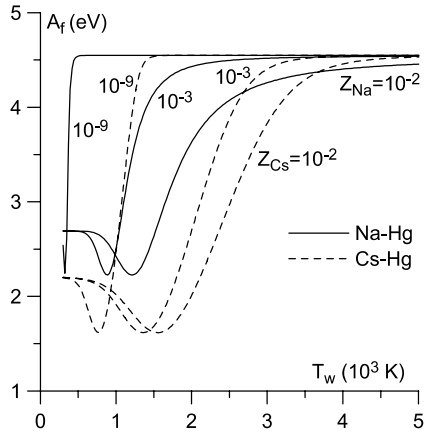

Figure 7. Work function of tungsten covered by a monolayer of Na or Cs in Na–Hg or Cs–Hg plasmas. $p = 5$ bar.

Calculated dependence of the work function of tungsten covered by a monolayer of Na or Cs on the surface temperature is shown in figure 7 for different molar fractions of the alkali metal. One can see that even small amounts of the alkali vapour in the plasma, of the order of 1% and less, can produce a significant effect on the work function. It should be emphasized that the decrease in the work function produced by adding Cs to the mercury plasma is stronger than that produced by adding Na and comes into play at higher values of the surface temperature.

4. Modelling diffuse discharge on tungsten cathodes

4.1. Effect of presence of MHs in the near-cathode plasma layer

In order to identify effects caused by variation of properties of the near-cathode plasma layer owing to the presence of MHs in the gas phase, let us consider results of simulations performed for the MH plasma under the assumption of a clean tungsten cathode, i.e. with a fixed value of the work function equal to 4.55 eV. The dependence of the density q of the energy flux from the MH plasma to the cathode surface on the surface temperature T_w at a fixed value of the near-cathode voltage drop U for two values of U is shown in figure 8. Also shown are data for the pure mercury plasma. One can see that the two dependences are not very different, however, the energy flux density at T_w around 3000 K is somewhat higher in the case of the MH plasma.

Results of calculations of diffuse current transfer from the MH plasma to a clean tungsten cathode are shown in figure 9. These calculations, as well as the following ones, have been performed for a cathode in the form of a rod of radius $R = 1$ mm and of height $h = 14.5$ mm; a geometry convenient for purposes of illustration. The data shown in the figure include the maximum temperature of the cathode surface (which is attained at the edge of the front surface, as in the case of a single-species plasma-producing gas [4]) and the corresponding dependence of the near-cathode voltage drop U on the arc current I, i.e. the current–voltage characteristic of the diffuse mode. Also shown are data for the pure mercury

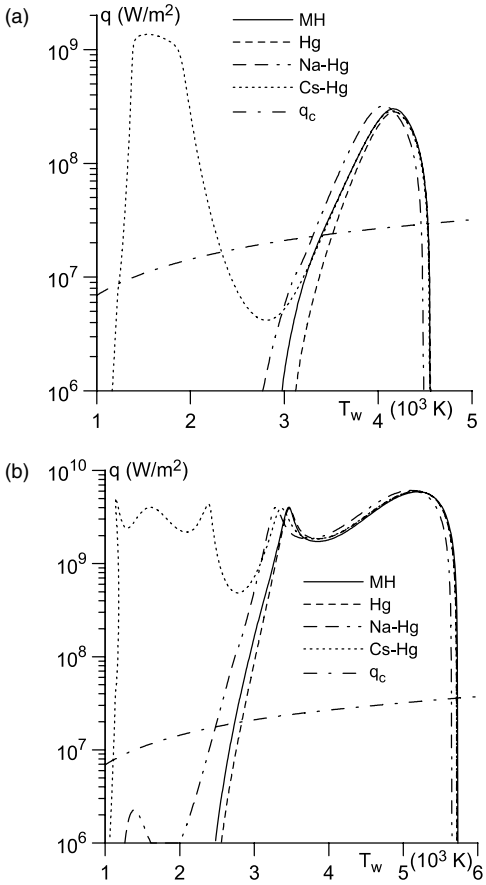

Figure 8. Dependence of the energy flux density from different plasmas to the surface of a tungsten cathode on the surface temperature. $p = 5$ bar. MH plasma: Hg : Na : Tl : I = 0.89 : 0.005 : 0.05 : 0.055, clean cathode. Na–Hg plasma: $Z_{Na} = 1\%$, cathode covered by a monolayer of Na. Cs–Hg plasma: $Z_{Cs} = 0.3\%$, cathode covered by a monolayer of Cs. (*a*) $U = 10$ V. (*b*) $U = 50$ V.

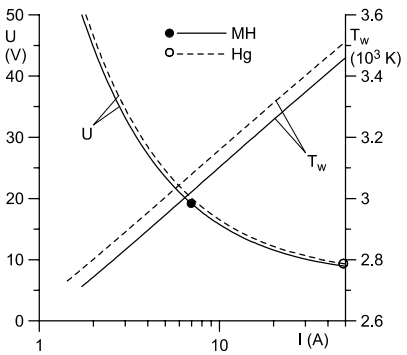

Figure 9. Maximal temperature of the cathode surface in the diffuse mode, current–voltage characteristics and the stability limit (points) of the diffuse mode of discharge on a clean tungsten cathode. MH plasma: Hg : Na : Tl : I = 0.89 : 0.005 : 0.05 : 0.055. $p = 5$ bar.

plasma. One can see that an addition of MHs to mercury results in a small decrease of the cathode surface temperature and of the near-cathode voltage drop. Note that this effect stems from the above-mentioned fact that the energy flux density at T_w around 3000 K is somewhat higher in the case of the MH plasma.

Points in figure 9 represent values of the limit of stability of the diffuse mode, i.e. the current value below which the diffuse discharge becomes unstable against the first mode of three-dimensional perturbations. (These values have been calculated by means of analysis of stability against the first mode of three-dimensional perturbations of axially symmetric temperature distributions in an axially symmetric body heated by a nonlinear external energy flux as described in [1,6].) One can see that the presence of MHs in the gas phase results in an expansion of the range of stability of the diffuse mode. This effect is due to the presence of species with strongly different ionization potentials in the gas phase and is discussed in detail elsewhere [16].

4.2. Effect of formation of a monolayer of alkali atoms on the cathode surface

Let us proceed to effects caused by a variation of the work function of the cathode surface owing to formation of a monolayer of alkali metal atoms on the surface. The density of energy flux from the Na–Hg plasma with $Z_{Na} = 1\%$ and from the Cs–Hg plasma with $Z_{Cs} = 0.3\%$, calculated accounting for variation of the work function due to formation of a monolayer of Na or, respectively, Cs atoms on the surface, is shown in figure 8. In the range $T \gtrsim 3000$ K, densities of energy flux from the Na–Hg and Cs–Hg plasmas are not very different from those from the Hg and MH plasmas. A qualitative difference can be seen at lower temperatures in the case of the Cs–Hg plasma: one or more new maxima appear. A similar but weaker effect appears also in the case of the Na–Hg plasma; note that at $U = 10$ V there is a maximum in the vicinity of the point $T_w = 1360$ K, however, this maximum is too low to be seen on the graph (the corresponding value of q is about 2.2×10^4 W m^{-2}).

Furthermore, the dotted curve in the figure 8(*b*) representing the first growing section of the dependence of q on T_w for the Cs–Hg plasma is S-shaped, although the range of T_w in which the S-shape occurs (i.e. in which the dependence of q on T_w is three-valued) is rather narrow, $1140 \lesssim T_w \lesssim 1190$ K, and the S-shape is hardly visible. In fact, such an S-shape occurs at all values of U exceeding approximately 15 V.

It should be emphasized that the appearance of the new maxima and of the S-shape is entirely due to the variation of the work function, since calculations for the Na–Hg and Cs–Hg plasmas with the fixed value of the work function equal to 4.55 eV, which are not shown on the graph, gave dependences similar to those for the pure mercury plasma.

In order to understand the changes of the diffuse mode of current transfer that can be caused by the appearance of the above-mentioned maximum or maxima, it is convenient to resort to the one-dimensional model of the cathode [1]. That is, let us for a moment consider a rod cathode with a thermally and electrically insulated lateral surface. Thermal balance of such cathode is governed by the equation $q(T_w, U) = q_c(T_w)$, where $q(T_w, U)$ is the density of the energy flux from the plasma to the cathode surface as before and

$$q_c(T_w) = \frac{1}{h}\int_{T_c}^{T_w} \kappa(T)\,\mathrm{d}T \qquad (1)$$

is the density of energy flux removed from the cathode top by thermal conduction to the bottom. (Here κ is thermal conductivity of the cathode material and T_c is the temperature of the bottom, which is assumed to be equal to 293 K in this work.) The dependence $q_c(T_w)$ for a tungsten cathode of height $h = 14.5$ mm is shown in figure 8. One can see that the equation $q(T_w, U) = q_c(T_w)$ for the Cs–Hg plasma at $U = 10$ V has four roots. In other words, four different one-dimensional thermal regimes are possible at $U = 10$ V. It follows that, while the current–voltage characteristics $U(I)$ of the diffuse mode in the case of Hg, MH and Na–Hg plasmas consist of two branches separated by a minimum [1], the characteristic of diffuse discharge in the Cs–Hg plasma consists of four branches separated by two minima and a maximum.

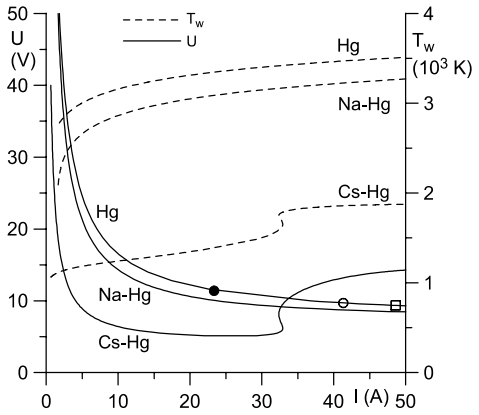

Figure 10. Lines: maximal temperature of the cathode surface in the diffuse mode and current–voltage characteristics of the diffuse mode of discharge on a tungsten cathode. Na–Hg plasma: $Z_{Na} = 1\%$, cathode covered by a monolayer of Na. Cs–Hg plasma: $Z_{Cs} = 0.01\%$, cathode covered by a monolayer of Cs. Points: stability limit of the diffuse mode in the Na–Hg plasma with $Z_{Na} = 0.08\%$ on the cathode covered by a monolayer of Na (●); in the Na–Hg plasma with $Z_{Na} = 0.08\%$ on the clean cathode (○); in the Hg plasma (□). $p = 5$ bar.

Since an increase in the work function with an increase of the surface temperature may render non-monotonic the dependence of emission current on the surface temperature, more than one diffuse-mode solution may correspond to the same arc current. In other words, the current–voltage characteristic $U(I)$ of the diffuse mode may become S-shaped.

Thus, one can expect that the variation of the work function caused by a monolayer of alkali atoms does not change qualitatively the diffuse mode of current transfer in the Na–Hg plasma but may affect dramatically the diffuse mode of current transfer in the Cs–Hg plasma.

The reasoning of the preceding paragraphs applies to a cathode with thermally and electrically insulated lateral surface. Results of two-dimensional simulations taking into account the current and energy collection by the lateral surface are shown in figure 10. Note that the difference between the dependences $T_w(I)$, $U(I)$ for the Na–Hg and Cs–Hg plasmas, on the one hand, and the similar dependences for the pure mercury plasma, on the other, is almost entirely due to the variation of the work function. (Calculations for the Na–Hg and Cs–Hg plasmas with the fixed value of the work function equal to 4.55 eV, which are not shown on the graph, gave dependences very close to those for the pure mercury plasma.)

One can see from figure 10 that in the case of the Na–Hg plasma the variation of the work function causes a decrease

in the cathode surface temperature and in the near-cathode voltage drop. In other words, formation of the sodium monolayer on the surface affects current transfer in the same direction that the presence of sodium in the gas phase does but produces a somewhat stronger effect. In general, formation of the sodium monolayer affects interaction of the Na–Hg plasma with a thermionic cathode only moderately.

On the contrary, there is a striking difference between the dependences $T_w(I)$, $U(I)$ for the Cs–Hg plasma and those for the pure mercury plasma. The temperature of the cathode surface decreases quite significantly: at currents of the order of 1 A, it is slightly above 1000 K. The current–voltage characteristic $U(I)$ is S-shaped (i.e. the dependence of U on I is three-valued) at currents between approximately 32 and 33 A. A similar S-shape is present also in the dependence $T_w(I)$. In accordance with to the earlier discussion, these S-shapes result from the non-monotonic dependence of emission current on the surface temperature (which, in turn, results from the increase in the work function with the surface temperature) and are unrelated to the S-shape shown in figure 8(*b*), which occurs at near-cathode voltages and/or cathode surface temperatures higher than those encountered in the calculations represented in figure 10. Note that the maximum and the second minimum of the current–voltage characteristic predicted above on the basis of the one-dimensional model have been revealed also by the two-dimensional simulation being described, however they are positioned at high currents far beyond the range covered by figure 10.

The complete current–voltage characteristic of the cathodic part of the discharge includes also the branch coinciding with the positive part of the axis of voltages, which describes the situation where no arc is present. Therefore, the complete current–voltage characteristic of the diffuse mode on clean cathodes includes three branches: the branch coinciding with the positive part of the axis of voltages, the falling section of the dependence $U(I)$ describing the diffuse discharge (this section can be seen, e.g. in figure 9), and the growing section of the dependence $U(I)$ describing the diffuse discharge (which occurs at currents higher than those represented in figure 9). In other words, the complete current–voltage characteristic of the diffuse mode on clean cathodes is N-shaped, which is essential for understanding the spot modes [1]. In such terms, the current–voltage characteristic of the diffuse mode in the Cs–Hg plasma shown in figure 10 should be called N–S-shaped.

It is interesting that at $I \gtrsim 34$ A the near-cathode voltage drop in the Cs–Hg plasma exceeds that in the pure Hg plasma. In order to understand the reason, let us consider distributions of the temperature along the cathode surface for the cases of the Cs–Hg and pure Hg plasmas which are shown in figure 11 for two values of the arc current, $I = 10$ A and $I = 40$ A. Here, r and z are cylindrical coordinates with the origin at the centre of the front surface of the cathode and with the z-axis directed from the front surface into the cathode body. In accord with this choice, $\{r \leqslant R, z = 0\}$ is the (circular) front surface of the cathode while $\{r = R, z \geqslant 0\}$ is the (cylindrical) lateral surface, so the range $0 \leqslant r + z \leqslant R$ in figure 11 corresponds to the front surface while the range $r + z \geqslant R$ corresponds to the lateral surface. (We recall here

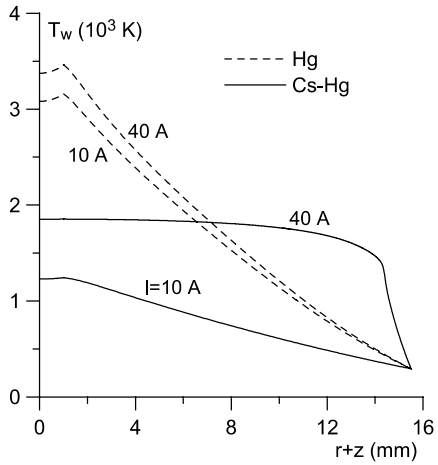

Figure 11. Temperature distribution over the cathode surface. $p = 5$ bar. Cs–Hg plasma: $Z_{Cs} = 0.01\%$, cathode covered by a monolayer of Cs.

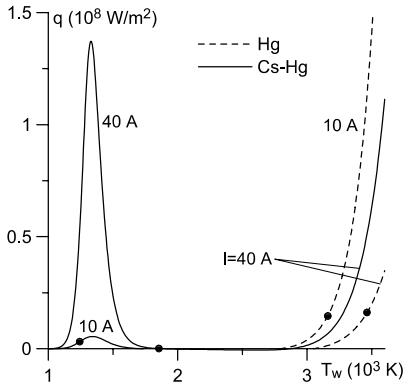

Figure 12. Dependence of the energy flux density to the cathode surface on the surface temperature. $p = 5$ bar. Cs–Hg plasma: $Z_{Cs} = 0.01\%$, cathode covered by a monolayer of Cs. Points: maximal temperature of the cathode surface.

that $R = 1$ mm in these calculations.) In the case of Hg plasma, the temperature distribution along the cathode surface is non-monotonic with the hottest point at the edge of the front surface, where conditions for thermal-conduction heat removal are the worst. The temperature does change much along the front surface of the cathode and decreases nearly linearly along the lateral surface. These distributions are similar to those established in [4] and are typical of the diffuse discharge on a thin cathode operating on the falling section of the current–voltage characteristic or, in other words, on the (first) growing section of the dependence of q on T_w.

In the case of the Cs–Hg plasma, the temperature distribution at $I = 10$ A is similar to that for the Hg plasma. At $I = 40$ A, the distribution is strongly different: the temperature is nearly constant at all points of the cathode surface except at a small section of the lateral surface adjacent to the bottom, where T_w rapidly falls to the bottom temperature. This distribution is typical of the diffuse discharge operating on the growing section of the current–voltage characteristic or, in other words, on the falling section of the dependence of q on T_w [5].

The dependence of q on T_w for the cases of the Cs–Hg and pure Hg plasmas is shown in figure 12. The near-cathode

voltage was set equal to approximately 6.4 and 12.9 V in the case of the Cs–Hg plasma and to approximately 16.5 V and 9.8 A in the case of the pure Hg plasma; in both cases these values correspond to $I = 10$ A and $I = 40$ A, respectively. The points in this figure indicate the maximum temperature of the cathode surface in each case. One can see that the discharge indeed operates on the growing section of the dependence of q on T_w in the case of the pure Hg plasma and in the case of the Cs–Hg plasma at $I = 10$ A and on the falling section of the dependence of q on T_w in the case of the Cs–Hg plasma, at $I = 40$ A. Note that the function q in the case of the Cs–Hg plasma at $I = 40$ A takes negative values in the range $1890\,\text{K} \lesssim T_w \lesssim 2870\,\text{K}$, although these values are small and barely visible on the graph. According to the general theory [5], the maximum temperature of the cathode surface cannot take values within this range. Indeed, the maximum temperature of the cathode surface found in the calculation, which is equal to 1850 K, is slightly below this range.

Thus, the reason why the near-cathode voltage drop in the Cs–Hg plasma at $I \gtrsim 34$ A exceeds that in the pure Hg plasma has been found: the discharge in this current range operates on the growing section of the dependence of q on T_w in the case of the pure Hg plasma and on the falling section in the case of the Cs–Hg plasma.

Also shown in figure 10 is the limit of stability of the diffuse mode in the Na–Hg plasma against the first mode of three-dimensional perturbations, calculated as described in [1, 6] for $Z_{Na} = 0.08\%$, with and without accounting for the variation of the work function, and in the pure mercury plasma. In calculations taking into account, of the variation of the work function at $Z_{Na} \gtrsim 0.09\%$, the instability disappears, i.e. the diffuse mode becomes stable at all currents against the first mode of three-dimensional perturbations. (Note that the disappearance of the instability against the first mode of three-dimensional perturbations was first detected in calculations with a clean cathode and analysed in detail in [16], however, on a clean cathode it occurs at higher Z_{Na}.) One can conclude that the presence of sodium in the gas phase results in an expansion of the range of stability of the diffuse mode (cf discussion of figure 9); the formation of sodium monolayer on the surface produces a similar but somewhat stronger effect.

As far as stability of the diffuse mode in the Cs–Hg plasma is concerned, it is unclear whether the approach [1, 6] can be applied directly, given the complex form of the current–voltage characteristic of the Cs–Hg plasma shown in figure 10. Therefore, the question of stability of the diffuse mode in the Cs–Hg plasma requires an additional mathematical treatment and falls beyond the scope of this work.

5. Concluding remarks

Addition of MHs to mercury affects the current transfer to thermionic cathodes in two ways: through variation of properties of the near-cathode plasma layer owing to the presence of MHs in the gas phase; and through variation of the work function of the cathode surface owing to formation of an alkali metal monolayer on the surface. Both effects are dealt with in this work. Methods of accounting for these effects are developed and implemented as parts of a general code describing interaction of thermionic cathodes with high-pressure plasmas. The main features of current transfer to cathodes under conditions characteristic of MH lamps are studied by means of numerical simulation with the use of the code developed.

Species taken into account by the developed model of the near-cathode plasma layer in an MH plasma comprise Hg, Na, Tl, Cs, Dy, Sc, I, NaI, TlI, CsI, DyI, DyI_2, DyI_3, ScI, ScI_2, ScI_3, Hg^+, Na^+, Tl^+, Dy^+, Sc^+, Cs^+, I^+, I^-. The model includes, in particular, an account of dissociation of metal iodide molecules by impact of both neutral particles and electrons. Results of calculations of the plasma composition, of individual and effective rate constants of ionization of a neutral particle by electron impact, and of individual and effective mean cross-sections for momentum transfer in elastic collisions between a positive ion and a neutral particle are presented. Calculations of diffuse discharge on tungsten cathodes in the MH plasma show that the presence of MHs in the gas phase results in a small decrease in the cathode surface temperature and in the near-cathode voltage drop and in an expansion of the range of stability of the diffuse mode.

Effects caused by a variation of the work function of the cathode surface owing to formation of a monolayer of alkali metal atoms on the surface are studied for particular cases where the plasma-producing gas contains mercury and sodium or caesium. In the case of the Na–Hg plasma, formation of the sodium monolayer affects the diffuse mode of current transfer in the same direction that the presence of metal atoms in the gas phase does, i.e. the cathode surface temperature and the near-cathode voltage drop decrease weakly while the range of stability of the diffuse mode expands. In general, formation of the sodium monolayer affects the plasma–cathode interaction only moderately. On the contrary, formation of the caesium monolayer changes the plasma–cathode interaction dramatically: the temperature of the cathode surface decreases very strongly and the diffuse-mode current–voltage characteristic becomes N–S-shaped.

In order to check, experimentally, theoretical conclusions of this work on the stability range of the diffuse mode, observations of the diffuse-spot transitions occurring on arc cathodes with decreasing current are needed. In other words, an experiment should start at high dc currents, where the diffuse discharge is stable, and the current should gradually decrease until the discharge switches into a spot mode. Unfortunately, such experiments with MH plasmas have not been conducted, hence, a comparison with the experiment can only be indirect.

The conclusion on expansion of the range of stability of the diffuse mode made in this work for the case of the Na–Hg plasma conforms to the general trend that cathode spots are not typical for high-pressure sodium lamps. In recent experiments [10], a dc discharge in the pure Hg plasma on 180 μm radius tungsten rod cathodes in the current range 0.3–0.7 A operated in the diffuse mode. An addition of unspecified amounts of NaI and TlI resulted in a small decrease in the cathode temperature; the discharge still operated in the diffuse mode. Obviously, this finding does not contradict the theoretical results of this work as far as the effect of sodium is concerned.

The discharge [10] operated in the spot mode when NaI, TlI and DyI were added. This finding, however, cannot be

confronted with this results since the conclusion on expansion of the range of stability of the diffuse mode was drawn in this work for the case of the Na–Hg plasma; in other cases, the situation may be much more complicated as shown by the example of the Cs–Hg plasma. Besides, the fact that the spot mode appears in the experiment does not necessarily mean that the diffuse mode is unstable: it may be that both modes are stable in the current range considered and which, one realizes, depends on other factors as well.

Acknowledgments

The work was performed within activities of the project *NumeLiTe* of the 5th Framework programme ENERGIE of the EC, of the project POCTI/FIS/60526/2004 of FCT and FEDER, and of the action 529 of the programme COST of the EC.

References

[1] Benilov M S 1998 *Phys. Rev.* E **58** 6480–94
[2] Bötticher R and Bötticher W 2000 *J. Phys. D: Appl. Phys.* **33** 367–74
[3] Bötticher R and Bötticher W 2001 *J. Phys. D: Appl. Phys.* **34** 1110–5
[4] Benilov M S and Cunha M D 2002 *J. Phys. D: Appl. Phys.* **35** 1736–50
[5] Benilov M S and Cunha M D 2003 *J. Phys. D: Appl. Phys.* **36** 603–14
[6] Benilov M S and Cunha M D 2003 *Phys. Rev.* E **68** 056407-1-11
[7] Bötticher R, Graser W and Kloss A 2004 *J. Phys. D: Appl. Phys.* **37** 55–63
[8] Dabringhausen L 2004 Charactrerization of electrodes of high-pressure plasma lamps by means of pyrometry and simulation *PhD Thesis* Tenea Verlag, Berlin (in German)
[9] Galvez M 2005 *J. Phys. D: Appl. Phys.* **38** 3011 (this issue)
[10] Luijks G M J F, Nijdam S and v Esveld H A 2005 *J. Phys. D: Appl. Phys.* **38** 3163 (this issue)
[11] Lichtenberg S, Dabringhausen L, Mentel J and Awakowicz P 2004 *Light Sources 2004 (Proc. 10th Int. Symp. on Science and Technology of Light Sources, Toulouse, 18–22 July 2004) Institute of Physics Conference Series* vol 182, ed G Zissis (Bristol: Institute of Physics Publishing) pp 609–10
[12] Paul K C, Erraki A, Takemura T, Hiramoto T, Dawson F, Rouffet J B, Gonzalez J J, Gleizes A and Lavers D 2004 *Light Sources 2004 (Proc. 10th Int. Symp. on Science and Technology of Light Sources, Toulouse, 18–22 July 2004) Institute of Physics Conference Series* vol 182, ed G Zissis (Bristol: Institute of Physics Publishing) pp 491–2
[13] Nandelstädt D, Redwitz M, Dabringhausen L, Luhmann J, Lichtenberg S and Mentel J 2002 *J. Phys. D: Appl. Phys.* **35** 1639–47
[14] Benilov M S and Marotta A 1995 *J. Phys. D: Appl. Phys.* **28** 1869–82
[15] http://www.arc_cathode.uma.pt
[16] Benilov M S, Cunha M D and Naidis G V 2005 *Plasma Sources Sci. Technol.* **14** 517–24
[17] Biberman L M, Vorob'ev V S and Yakubov I T 1987 *Kinetics of Nonequilibrium Low-Temperature Plasma* (New York: Plenum)
[18] Almanstötter J, Eberhard B, Günther K and Hartmann T 2002 *J. Phys. D: Appl. Phys.* **35** 1751–6
[19] Welton R F 2002 http://it.sns.ornl.gov/asd/public/pdf/sns0014/sns0014.pdf